Delaunay surfaces of prescribed mean curvature in Berger spheres

Antonio Bueno

Departamento de Ciencias, Centro Universitario de la Defensa de San Javier, E-30729 Santiago de la Ribera, Spain.
E-mail address: antonio.bueno@cud.upct.es

Abstract

We obtain a classification result for rotational surfaces in Berger spheres, whose mean curvature is given as a prescribed function of their angle function. Under hypothesis on the prescribed function, we show that these surfaces behave like the Delaunay surfaces of constant mean curvature. The classification is done by means of a phase plane analysis of the ODE fulfilled by the profile curve of such surfaces.

1 Introduction

The theory of positive, constant mean curvature (CMC) surfaces in homogeneous 3-spaces has been an active field of research in the past decades. A major achievement was the definition by Abresch and Rosenberg [AbRo] of a holomorphic quadratic differential in any CMC surface, that vanishes on rotational examples. Conversely, a CMC surface with vanishing *Abresch-Rosenberg differential* must be rotational. This resolution of the Hopf problem attracted the attention of many researches, producing a vast literature regarding this field of research; see e.g. [Dan, DHM, dCFe, FeMi] and subsequent works.

An important geometric problem is to classify CMC surfaces invariant by a 1-parameter group of isometries. We highlight the works of [FMP, Gor, HsHs, PeRi, Tom, Tor], where the authors achieved, among other important results, the classification of complete, rotational CMC surfaces in the $\mathbb{E}(\kappa,\tau)$ spaces: the homogeneous, simply connected, 3-dimensional manifolds whose isometry group have dimension 4. All the CMC surfaces in these spaces roughly follow the same pattern as the classical *Delaunay CMC surfaces* in $\mathbb{R}^3$: cylinders, spheres, unduloids and nodoids. In addition, rotational CMC tori appear as further examples in spaces of positive curvature.

Regarding more general curvature problems, in the past years the author started to focus on surfaces in $\mathbb{R}^3$ whose mean curvature is given as a prescribed function in the 2-sphere depending on the Gauss map, that is

$$H_\Sigma(p) = \mathcal{H}(N_p), \qquad \forall p \in \Sigma, \tag{1.1}$$

where $\mathcal{H} \in C^1(\mathbb{S}^2)$ and N is the Gauss map. For short, these surfaces are called $\mathcal{H}$-surfaces. Note that for the trivial case that $\mathcal{H}$ is a constant, we recover the CMC surfaces.

Mathematics Subject Classification: 53A10, 53C42, 34C05, 34C40
Keywords: Prescribed mean curvature; Berger sphere; Delaunay surfaces.

The existence and uniqueness of ovaloids satisfying (1.1) have their origins in the works of Alexandrov and Pogorelov [Ale, Pog], and more generally in the Minkowski problem [Min]. The author, jointly with Gálvez and Mira, started to develop the *global theory of surfaces with prescribed mean curvature* in [BGM1, BGM2], taking as main motivation the theory of CMC surfaces in $\mathbb{R}^3$. In particular, in [BGM1] the authors proved a classification result for rotational $\mathcal{H}$-surfaces for the particular case that Equation (1.1) is rotationally symmetric, that is

$$H_\Sigma(p) = \mathfrak{h}(\langle N_p, e_3\rangle), \qquad \forall p \in \Sigma,$$

where $\mathfrak{h} \in C^1([-1,1])$ and $\langle N, e_3\rangle$ is the angle function. Under necessary and sufficient conditions on $\mathfrak{h}$, the authors proved that rotational $\mathfrak{h}$-surfaces exhibit the same Delaunay pattern as CMC surfaces.

These works motivated to further investigate the properties of rotational $\mathfrak{h}$-surfaces [BuOr], and apply them to solve geometric problems [Bue1]. Also, the author generalized Equation (1.1) to more general ambient spaces. For that, take into account that the definition of the angle function can be done in any $\mathbb{E}(\kappa,\tau)$ space by measuring the projection of a unit normal vector field along a surface onto the unitary, vertical Killing vector field.

Definition 1.1 *Let be $\mathfrak{h} \in C^1([-1,1])$. We say that an oriented surface Σ in $\mathbb{E}(\kappa,\tau)$ is an $\mathfrak{h}$-surface if its mean curvature function H_Σ satisfies*

$$H_\Sigma(p) = \mathfrak{h}(\langle \eta_p, \xi\rangle), \qquad \forall p \in \Sigma, \tag{1.2}$$

where η is a unit normal along Σ and ξ is the vertical, unit Killing vector field of $\mathbb{E}(\kappa,\tau)$.

In analogy, these surfaces are called $\mathfrak{h}$-surfaces. Again, if $\mathfrak{h}$ is a constant, we have CMC surfaces in $\mathbb{E}(\kappa,\tau)$ spaces.

In the same fashion as for CMC surfaces, the author has recently achieved a Delaunay-type classification result for $\mathfrak{h}$-surfaces in the product spaces $\mathbb{M}^2(\kappa)\times\mathbb{R}$, in the Heisenberg space Nil_3 and the universal cover of the special linear group $\widetilde{SL_2}(\mathbb{R})$ [Bue2, Bue3]. Under hypotheses on the prescribed function, the complete, rotational $\mathfrak{h}$-surfaces in these spaces behave almost like their CMC counterparts. Surprisingly, in Nil_3 and $\widetilde{SL_2}(\mathbb{R})$ was proved the existence of rotational, embedded $\mathfrak{h}$-tori for some choices of the prescribed function, proving that rotational, embedded spheres are not unique in Alexandrov sense.

We emphasize in the fact that some hypothesis on the prescribed function must be imposed. For instance, if the mean curvature is a constant $H_0 > 0$, the Delaunay classification result holds if and only if

$$4H_0^2 + \kappa > 0.$$

For $\kappa > 0$ this inequality always holds, and for $\kappa = 0$ it just the fact that H_0 cannot vanish. However, for $\kappa < 0$ it reads as $H_0 > \sqrt{-\kappa}/2$. This value is known as the *critical value*: there exist CMC spheres if and only if $H_0 > \sqrt{-\kappa}/2$. Otherwise, entire graphs are the canonical rotational examples intersecting the axis of rotation.

A similar hypothesis was needed in [Bue2, Bue3] for the prescribed function; it was assumed to belong to the following space of functions:

$$\mathfrak{C}^1 := \{\mathfrak{h} \in C^1([-1,1]);\ \mathfrak{h}(y) = \mathfrak{h}(-y) > 0 \text{ and } 4\mathfrak{h}(y)^2 + \kappa(1-y^2) > 0,\ \forall y \in [-1,1]\}. \tag{1.3}$$

Note that if $\mathfrak{h} = H_0 > 0$, the fact that $H_0 \in \mathfrak{C}^1$ is just that H_0 is greater than the critical value.

In this paper we complete the Delaunay classification for $\mathfrak{h}$-surfaces in the $\mathbb{E}(\kappa,\tau)$ spaces, obtaining a similar pattern in the Berger spheres $\mathbb{S}^3_b(\kappa,\tau)$ as the one exhibited by [Tor]. The main result in this paper is the following:

Theorem 1.2 *Let be $\mathfrak{h} \in \mathfrak{C}^1$. Any complete, rotational $\mathfrak{h}$-surface in a Berger sphere is one of the following:*

1. *A torus with constant mean curvature $\mathfrak{h}(0)$.*
2. *An $\mathfrak{h}$-sphere with strictly monotone angle function.*
3. *A 1-parameter family of properly embedded $\mathfrak{h}$-unduloids.*
4. *A 1-parameter family of properly immersed (with self-intersections) $\mathfrak{h}$-nodoids.*
5. *An $\mathfrak{h}$-surface generated by rotating a union of curves meeting at a point of the antipodal fiber of the rotation axis.*

The arbitrariness of the prescribed function in (1.2) makes impossible to obtain a first integral just like in the CMC case. Even though we lack of having an explicit expression of the solutions, we analyze their behavior by means of the qualitative study of the phase plane of a non-linear autonomous system. This system is defined through the ODE fulfilled by the coordinates of the profile curve of a rotational $\mathfrak{h}$-surface.

The rest of the Introduction is devoted to detail the organization and structure of the paper.

In Section 2 we study the geometry of the Berger spheres. The main feature is the compactness of the space and to understand how the solutions may approach to a fiber antipodal to the fiber of rotation. In Section 2.1 we classify the $\mathbb{E}(\kappa,\tau)$ spaces, and in Section 2.2 we define a local coordinate model that describes the whole space $\mathbb{S}^3_b(\kappa,\tau)$ minus one fiber that is antipodal to the rotation fiber. We also recall the classification of rotational CMC surfaces in $\mathbb{S}^3_b(\kappa,\tau)$ obtained in [Tor].

In Section 3 we study rotational surfaces in Berger spheres. First, in 3.1 we deduce the differential equations that the profile curve of a rotational $\mathfrak{h}$-surface satisfies. In Section 3.2 we introduce the cornerstone of this study, the phase plane, and deduce some of its first properties. In Section 3.3 we further study the structure of the phase plane, how its solutions behave in it and the geometric implications on the underlying geometric problem.

Finally, in Section 4 we prove Theorem 1.2 by taking advantage of all the properties deduced of the phase plane. In Section 4.1 we discuss whether the rotational $\mathfrak{h}$-surfaces obtained are embedded or compact, in a similar fashion as in [Tor] for CMC surfaces.

Acknowledgments: The author is thankful to Francisco Torralbo for helpful comments and observations.

2 Geometry of the Berger spheres

2.1 The $\mathbb{E}(\kappa,\tau)$ spaces. Consider a homogeneous, simply connected, 3-dimensional manifold whose isometry group has dimension greater than 3. Moreover, suppose that is not a space form. Then, its isometry group has dimension 4 and is one of the $\mathbb{E}(\kappa,\tau)$ spaces for some $\kappa,\tau\in\mathbb{R}$ such that $\kappa\neq 4\tau^2$. A change in the orientation in the space changes τ into $-\tau$, hence we can suppose that $\tau\geq 0$ without losing generality. The $\mathbb{E}(\kappa,\tau)$ spaces admit a Riemannian submersion $\pi:\mathbb{E}(\kappa,\tau)\to\mathbb{M}^2(\kappa)$ onto the complete, simply connected surfaces of constant curvature κ, which has a unitary Killing vector field denoted by ξ whose integral curves are the fibers of the submersion.

The $\mathbb{E}(\kappa,\tau)$ spaces are classified as follows: if $\tau=0$ we recover the product spaces $\mathbb{M}^2(\kappa)\times\mathbb{R}$. When $\tau>0$ we get the Heisenberg space Nil_3 for $\kappa=0$; the universal cover of the special linear group $\widetilde{SL_2}(\mathbb{R})$ for $\kappa<0$; and the Berger spheres $\mathbb{S}^3_b(\kappa,\tau)$ for $\kappa>0$.

2.2 A local model. Consider the 3-dimensional sphere $\mathbb{S}^3:=\{(v,w)\in\mathbb{C}^2;\ |v|^2+|w|^2=1\}$ and the vector field $\widehat{\xi}=(iv,iw)$. Then, the Berger sphere $\mathbb{S}^3_b(\kappa,\tau)$ is $\mathbb{S}^3$ endowed with the metric

$$g(X,Y)=\frac{4}{\kappa}\left(\langle X,Y\rangle+\left(\frac{4\tau^2}{\kappa}-1\right)\langle X,\widehat{\xi}\rangle\langle Y,\widehat{\xi}\rangle\right),\qquad \forall X,Y\in T\mathbb{S}^3$$

where $\langle\cdot,\cdot\rangle$ is the flat metric in $\mathbb{C}^2$. In particular, when $\kappa=4\tau^2$ we recover the usual 3-sphere with a homothetic metric.

The Hopf fibration $\Pi:\mathbb{S}^3_b(\kappa,\tau)\to\mathbb{S}^2(\kappa)$

$$\Pi(v,w)=\frac{2}{\sqrt{\kappa}}\left(v\overline{w},\frac{1}{2}(|v|^2-|w|^2)\right),$$

is a Riemannian submersion whose kernel is precisely the vector field $\widehat{\xi}$ of constant length. Hence, Π is isomorphic to the canonical projection π of $\mathbb{E}(\kappa,\tau)$, and $\xi=\widehat{\xi}/|\widehat{\xi}|$ is the associated Killing vector field.

Now we describe a local coordinate model, which covers the whole $\mathbb{S}^3_b(\kappa,\tau)$ minus one fiber. Let us denote by $\mathcal{R}(\kappa,\tau)$ to $\mathbb{R}^3$ endowed with coordinates (x,y,z), and the metric

$$\langle\cdot,\cdot\rangle=\lambda^2(dx^2+dy^2)+(\lambda\tau(ydx-xdy)+dz)^2,\qquad \lambda=\frac{4}{4+\kappa(x^2+y^2)}. \tag{2.1}$$

Then, $\mathcal{R}(\kappa,\tau)$ is isometric to $\mathbb{S}^3_b(\kappa,\tau)$ and the Riemannian submersion π is isomorphic to the projection onto the first two coordinates. These two coordinates correspond to the inverse stereographic projection

$$\zeta(x,y)=\left(\lambda x,\lambda y,\frac{1}{\sqrt{\kappa}}(1-2\lambda)\right):\mathbb{R}^2\to\mathbb{S}^2(\kappa)-\{(0,0,1/\sqrt{\kappa})\},\qquad \lambda=\frac{1}{1+\frac{\kappa}{4}(x^2+y^2)}.$$

The third coordinate z of each point $(x,y,z)\in\mathcal{R}(\kappa,\tau)$ is the unit speed of the fiber $\Pi^{-1}(\zeta(x,y))$.

If we assume the axis of rotation in $\mathcal{R}(\kappa,\tau)$ to be the line $(0,0,z)$, then the fiber of rotation in $\mathbb{S}^3_b(\kappa,\tau)$ is $\Pi^{-1}(\zeta(0,0))=\Pi^{-1}((0,0,-1/\sqrt{\kappa}))$, that is the fiber $F:=(0,e^{i\theta}),\ \theta\in\mathbb{R}$. For

instance, the fiber in $\mathbb{S}^3_b(\kappa,\tau)$ that the model $\mathcal{R}(\kappa,\tau)$ omits is just $\Pi^{-1}((0,0,1/\sqrt{\kappa}))$, i.e. the fiber $F^* := (e^{i\theta},0),\ \theta\in\mathbb{R}$. An explicit local isometry between $\mathcal{R}(\kappa,\tau)$ and $\mathbb{S}^3_b(\kappa,\tau)-\{(e^{i\theta},0)\}$ is given by

$$\Psi(x,y,z)=\frac{1}{\sqrt{1+\frac{\kappa}{4}(x^2+y^2)}}\left(\frac{\sqrt{\kappa}}{2}(x+iy)e^{i\frac{\kappa}{4\tau}z},e^{i\frac{\kappa}{4\tau}z}\right). \tag{2.2}$$

With this isometry we see that two points (x,y,z) and $(x,y,z+8\tau\pi/\kappa)$ are identified to the same point in $\mathbb{S}^3_b(\kappa,\tau)$. A local inverse of Ψ between $\mathbb{S}^3_b(\kappa,\tau)-\{(e^{i\theta},0)\}$ and $\mathcal{R}(\kappa,\tau)$ is

$$\Psi^{-1}(v,w)=\left(\frac{2}{\sqrt{\kappa}|w|^2}Re(v\overline{w}),\frac{2}{\sqrt{\kappa}|w|^2}Im(v\overline{w}),\frac{4\tau}{\kappa}arg(w)\right).$$

Recall that if Σ is a surface in $\mathbb{S}^3_b(\kappa,\tau)$ invariant by the group of rotations *Rot* around the fiber $F=(0,e^{i\theta})$, then $\mathbb{S}^3_b(\kappa,\tau)/Rot$ is diffeomorphic to $\mathbb{S}^2$, and so Σ is just the image of a curve α in $\mathbb{S}^2$ under *Rot*. By rotational symmetry it suffices to just consider α in the half-sphere $\overline{\mathbb{S}^2_+}$, where $\partial\mathbb{S}^2_+=F$. For example, if $(w,a)\subset\mathbb{C}\times\mathbb{R}$ are the coordinates of a 2-sphere in $\mathbb{R}^3$, then the immersion

$$G:\mathbb{S}^2\to\mathbb{S}^3_b(\kappa,\tau),\ G(w,a)=(a,0,w)$$

is a minimal sphere whose equator $G(w,0)$ agrees with the fiber of rotation F. Hence, rotational surfaces in $\mathbb{S}^3_b(\kappa,\tau)$ are in correspondence with curves in the half-sphere $G(w,a),\ a\geq 0$. As a matter of fact, the profile curve of a rotational surface around F can be parametrized by $\alpha(s)=(\sin x(s),0,\cos x(s)e^{iz(s)})$.

Notice that the image of the set $G(\cos\theta,0,\sin\theta)$ under Ψ^{-1} is the line $(x,0,0),\ x>0$ for $\theta\in[0,\pi/2)$, and the line $(x,0,4\pi\tau/\kappa),\ x<0$ for $\theta\in(\pi/2,\pi]$. Finally, note that $G(0,0,1)=(1,0,0,0)\in F^*$ is the limit point $\lim_{x\to\infty}\Psi(x,0,0)$, and in general

$$\lim_{r\to\infty}\Psi(r\cos\theta_0,r\sin\theta_0,0)=\lim_{r\to\infty}\frac{1}{\sqrt{1+\frac{\kappa}{4}r^2}}\left(\frac{\sqrt{\kappa}}{2}re^{i\theta_0},1,0\right)=\left(e^{i\theta_0},0\right).$$

From now on, the point $p_N:=G(0,0,1)=(1,0,0,0)$ will be the *north pole* of $\mathbb{S}^3_b(\kappa,\tau)$.

The subset $\mathfrak{Z}$ in $\mathcal{R}(\kappa,\tau)$ such that $\Psi(\mathfrak{Z})$ lies in $G(\mathbb{S}^2)$ is the set of points $(x,y,z)\in\mathcal{R}(\kappa,\tau)$ such that $\Psi(x,y,z)\subset G(\mathbb{S}^2)=\{(a,0,w);\ a\in\mathbb{R},\ w\in\mathbb{C},\ a^2+|w|^2=1\}$ satisfy

$$x\sin\frac{\kappa z}{4\tau}+y\cos\frac{\kappa z}{4\tau}=0.$$

Thus, the orbit space in $\mathcal{R}(\kappa,\tau)$ that is identified with the orbit space $\overline{\mathcal{S}_+}\subset\mathbb{S}^3_b(\kappa,\tau)$ is a minimal helicoid. Since the helicoid and the xz-plane are 1-1 under the group of rotations leaving pointwise fixed the E_3-axis, such a plane will be considered to be the orbit space of rotational surfaces in $\mathcal{R}(\kappa,\tau)$.

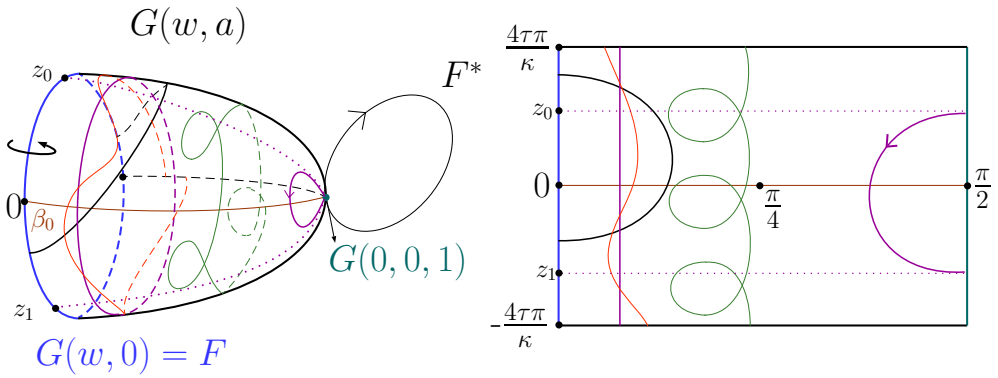

Figure 1: The profile curves of rotational CMC surfaces in Berger spheres $\mathbb{S}^3_b(\kappa,\tau)$.

As a matter of fact, the structure of the rotational surfaces with positive, constant mean curvature in $\mathbb{S}^3_b(\kappa,\tau)$ is represented in Figure 1. See [Tor] for a detailed description of these surfaces.

3 Rotational $\mathfrak{h}$-surfaces in Berger spheres

3.1 Basic formulas. We begin by locally parametrizing a rotational $\mathfrak{h}$-surface in the coordinate model $\mathcal{R}(\kappa,\tau)$. Let $\alpha(u)=(x(u),0,z(u))$ be a curve in the xz-plane. The map

$$\psi(u,\theta)=(x(u)\cos\theta, x(u)\sin\theta, z(u))\,,$$

defines an immersed surface Σ as the image of $\alpha(u)$ under the rotations of $\mathcal{R}(\kappa,\tau)$ around the axis $(0,0,z)$. The angle function of Σ in this model is

$$\nu=\frac{4x'}{\sqrt{16(1+\tau^2x^2)x'^2+z'^2(4+\kappa x^2)^2}},$$

and the mean curvature H_Σ has the following expression

$$2H_\Sigma=\frac{\left(4+\kappa x^2\right)^2\left(z'^3\left(16-\kappa^2x^4\right)-16z'\left(\tau^2x^3x''+xx''-x'^2\right)+16z''xx'\left(1+\tau^2x^2\right)\right)}{4x\left(z'^2\left(4+\kappa x^2\right)^2+16x'^2\left(1+\tau^2x^2\right)\right)^{3/2}}. \tag{3.1}$$

Now we consider the metric

$$d\sigma^2=(1+\tau^2x^2)dx^2+\frac{(4+\kappa x^2)^2}{16}dz^2 \tag{3.2}$$

in the xz-plane and the arc-length parameter s of α with respect to this metric (see Equation (2.8) in [GaMi]). A straightforward computation shows that with this arc-length parameter, the angle function is x' and the mean curvature is

$$2\varepsilon H_\Sigma=\frac{x\left(-x''\left(4+\kappa x^2\right)\left(1+\tau^2x^2\right)+xx'^2\left(\kappa-8\tau^2\right)-\kappa x\right)-4x'^2+4}{4x\sqrt{1-x'^2\left(1+\tau^2x^2\right)}},\qquad \varepsilon:=\operatorname{sign}(z'). \tag{3.3}$$

From now on we suppose that Σ is an $\mathfrak{h}$-surface for some $\mathfrak{h} \in C^1([-1,1])$, that is $H_\Sigma = \mathfrak{h}(x')$. Solving Equation (3.3) for x'' yields

$$x'' = \frac{4 - \kappa x^2 - x'^2(4 - x^2(\kappa - 8\tau^2)) - 8\varepsilon x \mathfrak{h}(x')\sqrt{1 - (1+\tau^2 x^2)x'^2}}{x\,(4+\kappa x^2)\,(1+\tau^2 x^2)}.$$

After the change of variable $x' = y$, this equation transforms into the first order, autonomous system

$$\begin{pmatrix} x \\ y \end{pmatrix}' = \begin{pmatrix} y \\ \dfrac{4 - \kappa x^2 - y^2(4 - x^2(\kappa - 8\tau^2)) - 8\varepsilon x \mathfrak{h}(y)\sqrt{1 - (1+\tau^2 x^2)y^2}}{x\,(4+\kappa x^2)\,(1+\tau^2 x^2)} \end{pmatrix}. \tag{3.4}$$

From the arc-length condition $(1+\tau^2x^2)x'^2 + (4+\kappa x^2)^2/16 z'^2 = 1$ we have that the angle function x' satisfies

$$x'^2 \leq \frac{1}{1+\tau^2 x^2},$$

with equality if and only if the height function z of α has a local extremum. This implies that system (3.4) is only defined for points (x_0, y_0) such that $x_0 > 0$ and $y_0^2 \leq 1/(1+\tau^2 x_0^2)$. For instance, note that since $\tau > 0$, the angle function satisfies $x' = \pm 1$ if and only if $x = 0$, which only happens at the axis of rotation.

3.2 The phase plane. The phase plane of Equation (3.4) is defined as the set

$$\Theta_\varepsilon := \left\{ (x,y);\ x > 0 \text{ and } y^2 < \frac{1}{1+\tau^2 x^2} \right\},$$

with coordinates (x, y) denoting the distance to the axis of rotation and the angle function. The boundary of Θ_ε consists of the segment $\{0\} \times [-1, 1]$ and the vertical graphs $y = \pm 1/\sqrt{1+\tau^2 x^2}$. We will denote by Ω^+ (resp. Ω^-) to the component $y = 1/\sqrt{1+\tau^2 x^2}$ (resp. to the component $y = -1/\sqrt{1+\tau^2 x^2}$), and by $\Omega := \Omega^+ \cup \Omega^-$.

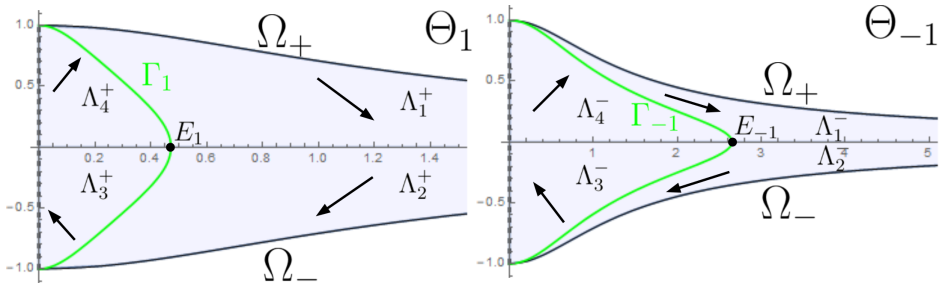

Figure 2: Left: the phase plane Θ_1, the curve Γ_1 and the equilibrium E_1. Right: the phase plane Θ_{-1}, the curve Γ_{-1} and the equilibrium E_{-1}. Both phase planes have their monotonicity regions and the behavior of an orbit at each region.

The orbits are the solutions of system (3.4) and will be denoted by $\gamma(s) = (x(s), y(s))$. The existence and uniqueness of the Cauchy problem associated to Equation (3.4) has as

consequence two important facts: *i*) two different orbits cannot intersect in Θ_ε, and *ii*) the orbits are a foliation of Θ_ε by regular C^1 curves.

Although we will remind it in the statement of the main results, **hereinafter $\mathfrak{h}$ will be always supposed to lie in the space $\mathfrak{C}^1$**; see Equation (1.3) for a definition of the space $\mathfrak{C}^1$.

Since $\mathfrak{h}$ is even, if $\gamma(s) = (x(s), y(s))$ is a solution to Equation (3.4), so it is $\widetilde{\gamma}(s) = (x(-s), -y(-s))$. Geometrically, this means that any orbit in the phase plane Θ_ε is symmetric with respect to the axis $y = 0$. This condition is related with the fact that rotations of angle π around horizontal geodesics send $\mathfrak{h}$-surfaces into $\mathfrak{h}$-surfaces.

A trivial solution to system (3.4) in Θ_1 is the one given by the constant orbit

$$E_1 = \left(\frac{2}{\sqrt{4\mathfrak{h}(0)^2 + \kappa} + 2\mathfrak{h}(0)}, 0 \right) = (e_1, 0). \tag{3.5}$$

This point is the *equilibrium* of (3.4) and generates a vertical cylinder in $\mathcal{R}(\kappa, \tau)$ which is identified with a compact torus in $\mathbb{S}^3_b(\kappa, \tau)$ of constant mean curvature equal to $\mathfrak{h}(0)$. These CMC tori are the inverse image of a circle in $\mathbb{S}^2$ by the Hopf fibration, and were called *Hopf tori* in [Tor].

The orbit in Θ_{-1} defined by

$$E_{-1} = \left(\frac{2}{\sqrt{4\mathfrak{h}(0)^2 + \kappa} - 2\mathfrak{h}(0)}, 0 \right) = (e_{-1}, 0) \tag{3.6}$$

is also a solution of Equation (3.4) for $\varepsilon = -1$. This point will be called the *equilibrium of* Θ_{-1}, and the $\mathfrak{h}$-surface generated by it is a Hopf torus in $\mathbb{S}^3_b(\kappa, \tau)$ of constant mean curvature equal to $\mathfrak{h}(0)$. Observe that the Hopf tori generated by the equilibria E_1, E_{-1} agree after an ambient isometry.

From Equation (3.4) we see that the points in Θ_ε with $y'(s) = 0$ are the ones lying in the intersection of Θ_ε with the (possibly disconnected) horizontal graph:

$$x = \Gamma_\varepsilon(y) := 2\sqrt{\frac{1 - y^2}{\kappa(1 - y^2) + 8(\mathfrak{h}(y)^2 + \tau^2 y^2) + 4\varepsilon\mathfrak{h}(y)\sqrt{4\mathfrak{h}(y)^2 + \kappa(1 - y^2) + 4\tau^2 y^2}}}. \tag{3.7}$$

We define $\Gamma_\varepsilon := \{x = \Gamma_\varepsilon(y)\} \cap \Theta_\varepsilon$. Note that the points lying in Γ_ε correspond to points whose angle function has vanishing derivative, and that $\Gamma_1 \cap \{y = 0\} = E_1$ and $\Gamma_{-1} \cap \{y = 0\} = E_{-1}$. Again, since $\mathfrak{h}$ is even we get that Γ_ε is symmetric with respect to the axis $y = 0$.

The curve Γ_ε and the axis $y = 0$ divide each Θ_ε into four connected components, Λ^ε_i, $i = 1, ..., 4$, called *monotonicty regions* where the coordinates $x(s)$ and $y(s)$ are strictly monotonous. The monotonicity at each region is detailed in the next proposition.

Proposition 3.1 *Let be $(x_0, y_0) \in \Theta_\varepsilon$ and consider an orbit $\gamma(s) = (x(s), y(s))$ such that $\gamma(s_0) = (x_0, y_0)$. Then, the following properties hold:*

1. *If $y_0 = 0$, then γ is orthogonal to the axis $y = 0$. If $y_0 \neq 0$, then we can see $\gamma(s)$ locally around $\gamma(s_0)$ as a graph $y(x)$. Then:*

2. *If $x_0 > \Gamma_\varepsilon(y_0)$ (resp. $x_0 < \Gamma_\varepsilon(y_0)$) and $y_0 > 0$, then $y(x)$ is strictly decreasing (resp. increasing) at x_0.*

3. *If $x_0 > \Gamma_\varepsilon(y_0)$ (resp. $x_0 < \Gamma_\varepsilon(y_0)$) and $y_0 < 0$, then $y(x)$ is strictly increasing (resp. decreasing) at x_0.*

4. *If $x_0 = \Gamma_\varepsilon(y_0)$, then $y'(x_0) = 0$ and $y(x)$ has a local extremum at x_0.*

Proof: First, we study how an orbit intersects the axis $y = 0$. Suppose that $\varepsilon = 1$ and let $\gamma(s) = (x(s), y(s))$ be an orbit in Θ_1 such that $\gamma(0) = (x_0, 0)$ for $x_0 > 0$. Moreover, suppose that $(x_0, 0)$ is not the equilibrium point. From Equation (3.4) we get

$$\gamma'(0) = \left(0, \frac{4 - x_0(8\mathfrak{h}(0) + \kappa x_0)}{x_0(4 + \kappa x_0^2)(1 + \tau^2 x_0^2)}\right).$$

So, $\gamma(0)$ intersects orthogonally $y = 0$, and it does either upwards or downwards depending on the sign of $p_\kappa(x_0)$, where $p_\kappa(x) = 4 - x(8\mathfrak{h}(0) + \kappa x)$. The zeroes of $p_\kappa(x)$ are

$$x_\pm = \frac{2}{2\mathfrak{h}(0) \pm \sqrt{4\mathfrak{h}(0)^2 + \kappa}},$$

that is,

$$x_+ = e_1, \qquad x_- = -e_{-1}.$$

Moreover, $p_\kappa(x) > 0$ if $x \in (x_-, x_+)$. Hence, if $x_0 < x_+ = e_1$ then $p_\kappa(x_0) > 0$ and $\gamma'(0)$ point upwards. Analogously, $\gamma'(0)$ points downwards when $x_0 > x_+ = e_1$.

By continuity and connectedness, and since $y'(s)$ only vanishes at points located at Γ_1, we have the following: the sign of $y'(s)$ of any orbit in $\Lambda_3^+ \cup \Lambda_4^+$ is also positive. The opposite holds for an orbit contained in $\Lambda_1^+ \cup \Lambda_2^+$, i.e. $y'(s)$ is negative. See Figure 2.

A similar argument works for the phase plane Θ_{-1}, concluding the proof. □

3.3 The structure of the phase plane. In the previous section we focused in how the orbits move through Θ_ε. In this section we exhibit further properties of the phase plane that determine the global and local behavior of an orbit $\gamma(s)$ as it approaches to some point, or tends to *escape* from Θ_ε.

We point out that since E_1 is a solution of Equation (3.4), because $\mathfrak{h} \in C^1$ and by uniqueness of the Cauchy problem, an orbit could converge to E_1 with the parameter $s \to \infty$. In fact, in [BGM1] we constructed explicit examples converging *directly* to E_1, that is without spiraling around it. However, this situation cannot happen if $\mathfrak{h}$ is even, as detailed next.

Proposition 3.2 *An orbit γ in Θ_ε cannot converge to E_ε.*

Proof: Let us analyze the structure of the orbits around E_1. The fact that $\mathfrak{h}$ is even implies that $\mathfrak{h}'(0) = 0$, and the linearized system of Equation (3.4) at E_1 is

$$\begin{pmatrix} u \\ v \end{pmatrix}' = \begin{pmatrix} 0 & 1 \\ F(\kappa, \tau, \mathfrak{h}(0)) & 0 \end{pmatrix} \begin{pmatrix} u \\ v \end{pmatrix},$$

where $F(\kappa, \tau, \mathfrak{h}(0))$ is a negative expression only depending on the mentioned variables; the fact that $\mathfrak{h} \in \mathfrak{C}^1$ is key here and in how the element a_{22} in the linearized matrix vanishes.

Hence, the orbits of the linearized system around the origin are ellipses, and by classical theory of non-linear autonomous systems we have two possible configurations around E_1: either the curves are closed, or they spiral around E_1, converging to it. However, the latter possibility cannot occur since the phase plane Θ_1 is symmetric with respect to $y = 0$, and E_1 belongs to this axis. In particular, all the orbits in Θ_1 stay at a positive distance from E_1.

The proof is analogous for the equilibrium E_{-1} of the phase plane Θ_{-1}. □

The following proposition restricts the limit points of an orbit in Θ_ε.

Proposition 3.3 *An orbit γ cannot converge to a point $(0, y) \in \overline{\Theta_\varepsilon}$, $|y| < 1$.*

Proof: Let $(x(s), y(s))$ be an orbit in Θ_1 such that $x(s) \to 0$ and $y(s) \to y_0 \in [-1, 1]$ as $s \to s_0$, and denote by $(x(s), z(s))$ to the coordinates of the profile curve associated to this orbit. Taking limit in Equation (3.2) when $s \to s_0$ we conclude that $x'(s)^2 + z'(s)^2 \to 1$.

Note that since $H_\Sigma = \mathfrak{h}(\nu)$, in particular H_Σ is bounded. Therefore, by taking limit in Equation (3.1) when $s \to s_0$ and after simplification, we arrive to

$$\lim_{s \to s_0} 2H_\Sigma(x(s), z(s)) = \lim_{s \to s_0} C_0 \frac{z'(s)}{x(s)} \qquad C_0 \in \mathbb{R}.$$

In conclusion, $\lim_{s \to s_0} z'(s) = 0$ in order to H_Σ not blowing up, and again by Equation (3.2) we conclude that $\lim_{s \to s_0} x'(s) = \lim_{s \to s_0} y(s) = \pm 1$. □

Geometrically, this implies that if an $\mathfrak{h}$-surface approaches or intersects the axis of rotation it does in an orthogonal way.

Recall that Equation (3.4) is singular at $x = 0$, hence we cannot ensure by standard theory the existence of rotational $\mathfrak{h}$-surfaces intersecting orthogonally the axis of rotation. However, this difficulty can be overcomed by invoking Lemma 4.1 in [GaMi], where the authors obtained a general existence result for radial solutions of a fully non-linear PDE in the $\mathbb{E}(\kappa, \tau)$ spaces. As a consequence, the two unique $\mathfrak{h}$-surfaces intersecting the axis of rotation with upwards and downwards orientation are defined next.

Definition 3.4 *Let be $\mathfrak{h} \in \mathfrak{C}^1$. We define the rotational $\mathfrak{h}$-surface Σ_+ (resp. Σ_-) as the unique $\mathfrak{h}$-surface intersecting orthogonally the axis of rotation with upwards (resp. downwards) orientation. Moreover, Σ_+ and Σ_- agree after a vertical translation and a rotation around a horizontal geodesic.*

The existence of Σ^+ and Σ^- has the following implications on the phase plane Θ_ε. See Corollary 2.4 in [BGM1] for further details.

Proposition 3.5 *There exists a unique orbit γ_+ (resp. γ_-) in Θ_1 having the point $(0,1)$ (resp. $(0,-1)$) in $\overline{\Theta_1}$ as endpoint. Moreover, γ_+ and γ_- are symmetric with respect to the axis $y=0$. There do not exist such orbits in Θ_{-1}.*

The following proposition studies the possible endpoints of an orbit in the boundary Ω of Θ_ε.

Proposition 3.6 *Let $\gamma(s)$ be an orbit in Θ_ε and consider $\alpha(s)=(x(s),0,z(s))$ the associated arc-length parametrized curve. Suppose that $\gamma(s)$ has some $(x_0,y_0)\in\Omega$ as endpoint at $s=s_0$. Then,*

1. *If $\gamma(s_0)\in\Omega^+$, $z(s)$ has a local minimum at $s=s_0$. In this case, $\gamma(s)$ lies in Θ_1 for $s>s_0$. For $s<s_0$, $\gamma(s)$ belongs to Θ_{-1}.*
2. *If $\gamma(s_0)\in\Omega^-$, $z(s)$ has a local maximum at $s=s_0$. In this case, $\gamma(s)$ lies in Θ_1 for $s<s_0$. For $s>s_0$, $\gamma(s)$ belongs to Θ_{-1}.*

Proof: Suppose that $\gamma(s_0)=(x_0,y_0)\in\Omega^+$ for some s_0 and let $\alpha(s)=(x(s),0,z(s))$ be the arc-length parametrized curve defined by $\gamma(s)$. Note that $x'(s_0)=y_0>0$. Because $\gamma(s_0)\in\Omega^+$ we have that the angle function $x'(s)=y(s)$ satisfies $y(s_0)=1/\sqrt{1+\tau^2x(s_0)^2}$, and thus the arc-length condition

$$(1+\tau^2x(s)^2)x'(s)^2+\frac{(4+\kappa x(s)^2)^2}{16}z'(s)^2=1$$

ensures us that $z'(s_0)=0$. From Equation (3.1) and the fact that $z'(s_0)=0$, we get

$$2\mathfrak{h}(x'(s_0))=\frac{\left(4+\kappa x(s_0)^2\right)^2 16x'(s_0)\left(1+\tau^2x(s_0)^2\right)}{4\left(16x'(s_0)^2\left(1+\tau^2x(s_0)^2\right)\right)^{3/2}}z''(s_0).$$

Since $\mathfrak{h}$ and $x'(s_0)=y(s_0)$ are positive, we see that $z''(s_0)$ is positive as well which yields that $z(s_0)$ is a local minimum of $z(s)$. Thus, $z(s)$ is increasing for $s>s_0$ and decreasing for $s<s_0$. This behavior implies that the orbit describing $\alpha(s)$ lies in Θ_1 for $s>s_0$ and in Θ_{-1} for $s<s_0$. Hence, this orbit in Θ_{-1} *ends* at $(x_0,y_0)\in\Omega^+$ and then *starts* at the same point but this time in Θ_1.

If $\gamma(s_0)\in\Omega^-$, the proof is similar; just note that $x'(s_0)=y_0<0$, hence $z''(s_0)$ is negative. This time, the orbit in Θ_1 *ends* at Ω^- and then *starts* at the same point but this time in Θ_{-1}. □

In any of these situations, i.e. where $z'(s)=0$ and it changes its monotony, we will say that the orbit in Θ_ε *continues* in $\Theta_{-\varepsilon}$. and this continuation has to be understood as the extension of the associated $\mathfrak{h}$-surface having a common point with the same unit normal.

Finally, we focus on whether an orbit can *escape* from the phase plane Θ_ε.

Theorem 3.7 *Let be $\mathfrak{h} \in \mathfrak{C}^1$ and $\gamma(s) = (x(s), y(s))$ an orbit in Θ_1. Then $x(s)$ cannot diverge to ∞.*

Proof: The proof will be done by contradiction. Let $\alpha(s) = (x(s), 0, z(s))$ be the arc-length parametrized curve generated by $\gamma(s)$. Then, the fact that $\alpha(s)$ is the profile of a rotational $\mathfrak{h}$-surface is equivalent to the following system to be fulfilled

$$\begin{cases} x'(s) = \dfrac{\cos\theta(s)}{\sqrt{1+\tau^2 x(s)^2}} \\ z'(s) = \dfrac{4\sin\theta(s)}{4+\kappa x(s)^2} \\ \theta'(s) = \dfrac{1}{(4+\kappa x(s)^2)\sqrt{1+\tau^2 x(s)^2}}\left(8\mathfrak{h}\left(\dfrac{\cos\theta(s)}{\sqrt{1+\tau^2 x(s)^2}}\right) - \dfrac{4-\kappa x(s)^2}{x(s)}\sin\theta(s)\right), \end{cases} \tag{3.8}$$

Here, $\theta(s)$ is the angle that $\alpha'(s)$ makes with the x-direction.

Now, suppose that $x(s) \to \infty$. By the structure and monotonicity of the phase plane, we may assume without losing generality that $\gamma(s)$ is strictly contained in Λ_1^+ and stays there as $x \to \infty$ (if γ stays in Λ_2^+ the proof is the same). In particular, $\theta(s) \to \pi/2$ holds. Now, we see the angle θ as a function of x; this can be done since $x'(s) > 0$ and by the inverse function theorem. Hence,

$$\theta'(s) = \frac{d\theta}{ds} = \frac{d\theta}{dx}\frac{dx}{ds} = \theta'(x)x'(s) = \theta'(x)\frac{\cos\theta(x)}{\sqrt{1+\tau^2x^2}}.$$

So, the third equation in (3.8) yields

$$\theta'(x)\cos\theta(x) = \frac{1}{x}\left(\frac{x}{4+\kappa x^2}8\mathfrak{h}\left(\frac{\cos\theta(x)}{\sqrt{1+\tau^2x^2}}\right) + \frac{\kappa x^2-4}{\kappa x^2+4}\sin\theta(x)\right) \geq \frac{c_0}{x}, \qquad c_0 > 0,$$

for $x > x_0$ and x_0 large enough. Integrating from x_0 and x we conclude $\sin\theta(x) \geq c_0 \log x + \sin\theta(x_0)$, which is a contradiction when $x \to \infty$. □

4 Proof of Theorem 1.2

In this section we prove Theorem 1.2. We will use the coordinate model $\mathcal{R}(\kappa, \tau)$ as introduced in Section 2, and suppose that the axis of rotation is the axis $(0, 0, z)$, $z \in \mathbb{R}$.

First, the equilibrium points E_1 and E_{-1} as defined in Equations (3.5) and (3.6) were showed to generate two Hopf tori of constant mean curvature equal to $\mathfrak{h}(0)$ that agree after an ambient isometry, proving the first item.

For the existence of the $\mathfrak{h}$-sphere, consider the orbit γ_+ starting at the point $(0, 1)$ at the instant $s = 0$ given by Proposition 3.5. For $s > 0$ small enough $\gamma_+(s)$ lies in Λ_1^+, and from Propositions 3.6 and 3.7 we conclude that $\gamma_+(s)$ is contained in Λ_1^+ until it intersects the axis $y = 0$ at some $\gamma(s_0) = (x_0, 0)$, $x_0 > 0$. This also holds for the orbit $\gamma_-(s)$, i.e. this time $\gamma_-(s)$ ends at the point $(0, -1)$ at some instant $s_1 > 0$, is contained in Λ_2^+ and comes from intersecting the axis $y = 0$ at a finite instant. Since γ_+ and γ_- are symmetric, they meet

orthogonally at the axis $y = 0$. By uniqueness γ_+ and γ_- can be smoothly glued to generate a compact orbit $\gamma_0 := \gamma_+ \cup \gamma_-$ that joins the points $(0, 1)$ and $(0, -1)$.

The arc-length parametrized curve $\alpha_0(s)$ associated to $\gamma_0(s)$ intersects the axis of rotation at the instant $s = 0$, has strictly increasing height function (hence is embedded in $\mathcal{R}(\kappa, \tau)$), and its angle function at the instant $s = s_0$ vanishes; here, the $x(s)$-coordinate reaches a global maximum and then decreases. By the even condition on $\mathfrak{h}$, α_0 is symmetric with respect to the horizontal geodesic at height $z(s_0)$ in the xz-plane. The $\mathfrak{h}$-surface generated by rotating α_0 is an $\mathfrak{h}$-sphere, denoted by $S_\mathfrak{h}$, with strictly decreasing angle function. See Figure 3.

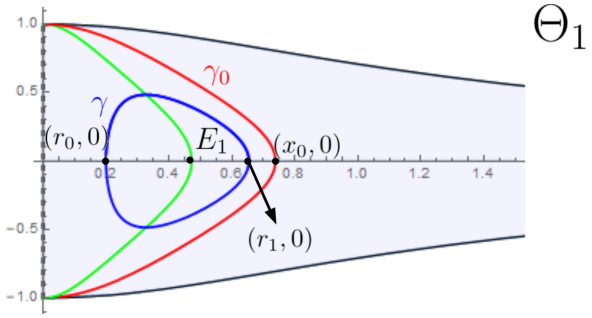

Figure 3: The phase plane Θ_1 for the Berger spheres. In red, the orbit γ_0 corresponding to the $\mathfrak{h}$-sphere. In blue, an orbit corresponding to an $\mathfrak{h}$-unduloid.

Recall that the orbit γ_0 of the $\mathfrak{h}$-sphere divides Θ_1 in two connected components: one bounded containing the equilibrium E_1, that we will denote by $\mathcal{W}_0$, and other unbounded that we will denote by $\mathcal{W}_\infty$.

To prove the existence of the $\mathfrak{h}$-unduloids, consider $r_0 > 0$ such that $(r_0, 0) \in \mathcal{W}_0$, and suppose that $(r_0, 0)$ is at the left-hand side of E_1. Let $\gamma(s) = (x(s), y(s))$ be the orbit passing through $(r_0, 0)$ at the instant $s = 0$. Then, for $s > 0$ small enough $\gamma(s)$ is contained in Λ_4^+ and follows its monotonicity direction. By continuity, $\gamma(s)$ has to intersect Γ_1 at some finite point, where the $y(s)$-coordinate of $\gamma(s)$ reaches a maximum, and then $\gamma(s)$ enters to the region Λ_1^+. Since $\gamma(s)$ cannot intersect γ_0 by uniqueness of the Cauchy problem and $\gamma(s)$ cannot converge to E_1 with $s \to \infty$ in virtue of Proposition 3.2, the only possibility for $\gamma(s)$ is to intersect the axis $y = 0$ at some finite point $\gamma(s_0) = (r_1, 0)$ lying at the right-hand side of E_1. By symmetry of Θ_1, the same behavior holds in the regions Λ_2^+ and Λ_3^+ and then $\gamma(s)$ reaches again the point $(r_0, 0)$ at some instant $s_1 > 0$, which implies that $\gamma(s)$ is a periodic orbit. Note that in any case, $\gamma(s)$ cannot converge to the segment $\{0\} \times [-1, 1]$ in virtue of Proposition 3.3.

This orbit generates an arc-length parametrized curve $\alpha(s)$ whose height function is strictly increasing (since $\gamma(s) \subset \Theta_1$) and hence $\alpha(s)$ is embedded in $\mathcal{R}(\kappa, \tau)$. The $x(s)$-coordinate of $\alpha(s)$ is periodic, its maximum is $x(s_0) = r_1$ and its minimum is $x(0) = r_0$; see Figure 3. The rotation of $\alpha(s)$ generates a properly embedded $\mathfrak{h}$-surface $U_\mathfrak{h}$ that is diffeomorphic to $\mathbb{S}^1 \times \mathbb{R}$ (in the model $\mathcal{R}(\kappa, \tau)$) and with periodic distance to the rotation axis, that is, $U_\mathfrak{h}$ is an $\mathfrak{h}$-unduloid. In Section 4.1 we discuss whether $U_\mathfrak{h}$ is compact, and hence is a torus, or not.

Moreover, each $\mathfrak{h}$-unduloid is uniquely determined by the value r_0 that agrees with the radius of the smallest circumference contained in $U_\mathfrak{h}$. Thus, the family of $\mathfrak{h}$-unduloids is a continuous family $\{U_\mathfrak{h}(r)\}$ parametrized by the *necksize* of their *waists*, where $0 < r < 2(\sqrt{4\mathfrak{h}(0)^2+\kappa}+2\mathfrak{h}(0))^{-1}$. Similarly to the CMC case, when $r \to 2(\sqrt{4\mathfrak{h}(0)^2+\kappa}+2\mathfrak{h}(0))^{-1}$ the $\mathfrak{h}$-unduloids $U_\mathfrak{h}(r)$ converge to the vertical cylinder of CMC $\mathfrak{h}(0)$, and when $r \to 0$ the $\mathfrak{h}$-unduloids converge to a singular chain of tangent $\mathfrak{h}$-spheres.

Next, we prove the existence of the $\mathfrak{h}$-nodoids. For that, let $(x_0, 0)$ be the point of intersection of γ_0 with $y = 0$, and fix some $w_0 > x_0$. Consider the orbit $\gamma(s)$ passing through $(w_0, 0)$ at the instant $s = 0$. For $s > 0$ small enough, $\gamma(s)$ lies in Λ_2^+, and since γ_0 and γ cannot intersect each other, $\gamma(s)$ has some $\gamma(s_0) = (w_1, y_1) \in \Omega^-$, $w_1 > 0$, $y_1 < 0$ as endpoint. By symmetry, $\gamma(s)$ for $s < 0$ has the same behavior at Λ_1^+, having the point $\gamma(-s_0) = (w_1, -y_1) \in \Omega^+$ as endpoint. This orbit generates an arc-length parametrized curve $\alpha(s)$ which is also symmetric with respect to the rotation of angle π around the horizontal geodesic in the xz-plane at height $z(0)$; after a vertical translation we can suppose that $z(0) = 0$. At this height, the $x(s)$-coordinate of $\alpha(s)$ reaches its maximum w_0, and then decreases to the value w_1. The height $z(s)$ reaches a minimum at $s = -s_0$ where $z'(-s_0) = 0$, then increases and reaches a maximum at $s = s_0$ where again $z'(s_0) = 0$.

Now, for $s > s_0$ the function $z(s)$ is decreasing, hence $\alpha(s)$ for $s > s_0$ generates an orbit $\sigma(s)$ in Θ_{-1} having the point $(w_1, y_1) \in \Omega^-$ as endpoint. The monotonicity properties of Θ_{-1} and Proposition 3.3 ensures us that $\sigma(s)$ has to intersect the axis $y = 0$ at some finite point $\sigma(s_1) = (\widehat{w_0}, 0)$, $\widehat{w_0} > 0$. By symmetry, $\sigma(s)$ ends up having the point $(w_1, -y_1) \in \Omega^+$ as endpoint for some $s = s_2$. Thus, the height of $\alpha(s)$ is strictly decreasing starting at the value $z(s_0)$ and having the value $z(s_2)$ as minimum. This time, the distance $x(s)$ to the axis of rotation has the value $\widehat{w_0}$ as minimum. See Figure 4.

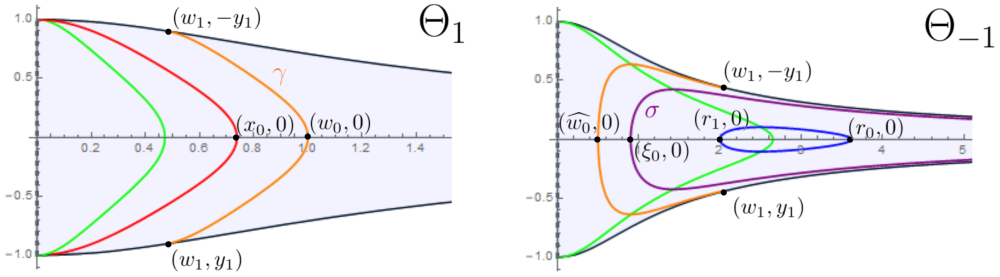

Figure 4: Left: the phase plane Θ_1 and an orbit in orange corresponding to an $\mathfrak{h}$-nodoid. Right: the phase plane Θ_{-1} with an orbit in orange corresponding to an $\mathfrak{h}$-nodoid, an orbit in blue corresponding to an $\mathfrak{h}$-unduloid, and the orbit in purple corresponding to the profile curve that passes through the north pole $p_N \in \mathbb{S}^3_b(\kappa, \tau)$ omitted in the model $\mathcal{R}(\kappa, \tau)$.

Finally, we analyze the case when a solution approaches to the fiber $F^* = (e^{i\theta}, 0)$ omitted by the model $\mathcal{R}(\kappa, \tau)$. Recall that the orbit γ_0 of the $\mathfrak{h}$-sphere intersects the axis $y = 0$ at $(x_0, 0)$. Consider an orbit γ in Θ_1 such that $\gamma(0) = (w_0, 0)$ with $w_0 > x_0$. This orbit corresponds to an $\mathfrak{h}$-nodoid, hence is compact and enters to the phase plane Θ_{-1} generating another compact orbit that intersects the axis $y = 0$ at some $(\widehat{w_0}, 0)$. Moreover, as w_0 increases $\widehat{w_0}$ also increases. Thus, when $w_0 \to \infty$ we conclude that $\widehat{w_0} \to w_\infty$ with $w_\infty \leq$

$2\left(\sqrt{4\mathfrak{h}(0)^2+\kappa}-2\mathfrak{h}(0)\right)^{-1}$, that is $(w_\infty,0)$ lies at the left-hand side of E_{-1} or agrees with it.

Now, take some $r_0>0$ and an orbit $\gamma\subset\Theta_{-1}$ such that $\gamma(0)=(r_0,0)$ lies at the right-hand side of E_{-1}. Then, γ is a closed orbit that has E_{-1} in its inner region, and thus generates an $\mathfrak{h}$-unduloid that agrees after an ambient isometry with an $\mathfrak{h}$-unduloid generated by an orbit in Θ_1. The orbit γ defines a unique point $(r_1,0)$, $r_1>0$ at the left-hand side of E_{-1} where γ intersects the $y=0$ axis. In particular, $r_1>w_\infty$ and so $(w_\infty,0)\neq E_{-1}$. Finally, recall that when r_0 increases then r_1 decreases and so $r_1\to r_\infty\geq w_\infty$ when $r_0\to\infty$.

By continuity of the phase plane, any orbit $\sigma(s)=(x(s),y(s))$ in Θ_{-1} passing through some $(\xi,0)$ with $\xi\in[w_\infty,r_\infty]$ is symmetric with respect to the axis $y=0$ and satisfies $x(s)\to\infty$ and $y(s)\to 0$ as $s\to\pm\infty$. This orbit generates a curve $\alpha(s)$ that starts from the north pole p_N of $\mathbb{S}^3_b(\kappa,\tau)$ at some instant $s=s_0<0$ with vanishing angle function, and ends again at p_N at $s=s_1>0$. Since $\alpha(s)$ is unique with this initial data, so it is σ in Θ_{-1}, i.e. $w_\infty=r_\infty:=\xi_0$. See Figure 4.

Let Σ be the $\mathfrak{h}$-surface generated by rotating $\alpha(s)$ around the fiber F. The fact that Σ is compact or embedded depends on whether the curve $\alpha(s)$ closes or not. For instance, when regarding $\alpha(s)$ in the model $\mathcal{R}(\kappa,\tau)$ name $z_0=\lim_{s\to-\infty}z(s)$ and $z_1=\lim_{s\to\infty}z(s)$ (see Figure 1). Then,

- If $z_0-z_1=4\pi\tau/\kappa$, then $\alpha'(s_0)=\alpha'(s_1)$ and so $\alpha(s)$ closes when reaching the north pole at the instant $s=s_1$. Hence, Σ is an embedded $\mathfrak{h}$-torus.
- If z_0-z_1 is a rational multiple of $4\pi\tau/\kappa$, then $\alpha'(s_0)\neq\alpha'(s_1)$ and so $\alpha(s)$ has a cusp at p_N. The different branches of $\alpha(s)$ are obtained by rotating $\alpha(s)$ an angle z_1-z_0 around p_N. After a finite number of iterations, $\alpha(s)$ closes and Σ is an immersed $\mathfrak{h}$-torus with self-intersections.
- If z_0-z_1 is an irrational multiple of $4\pi\tau/\kappa$, then $\alpha(s)$ never closes. Hence, Σ is an immersed, non-compact surface that is dense inside a solid torus.

4.1 Embeddedness and compactness of $\mathfrak{h}$-surfaces in $\mathbb{S}^3_b(\kappa,\tau)$. As pointed out in [Tor], CMC spheres in $\mathbb{S}^3_b(\kappa,\tau)$ might be either embedded or immersed and have self-intersections. As a matter of fact, if the difference of the heights between the top and bottom points is greater than $8\tau\pi/\kappa$, then the sphere has self-intersections. This is a consequence from the fact that in the model $\mathcal{R}(\kappa,\tau)$, two points (x,y,z) and $(x,y,z+8\tau\pi/\kappa)$ are identified to the same point in $\mathbb{S}^3_b(\kappa,\tau)$, see Equation (2.2).

The same happens for $\mathfrak{h}$-surfaces. If the height between the top and bottom points of an $\mathfrak{h}$-sphere is less than $8\tau\pi/\kappa$, then the $\mathfrak{h}$-sphere is embedded. Otherwise, it has self-intersections. Unlike CMC surfaces, no first integral is known for $\mathfrak{h}$-surfaces and so an explicit expression of the height of its solutions.

This discussion also holds regarding the compactness of $\mathfrak{h}$-unduloids and $\mathfrak{h}$-nodoids. If the difference of heights T between consecutive periodic points is a rational multiple of $8\tau\pi/\kappa$, these solutions close and hence generate compact $\mathfrak{h}$-tori. Moreover, they are embedded if and

only if $T = \frac{8\tau\pi}{p\kappa}$, $p \in \mathbb{Z}$. Finally, if T is an irrational multiple of $8\tau\pi/\kappa$ then the corresponding $\mathfrak{h}$-unduloid or $\mathfrak{h}$-nodoid never closes, hence is not compact and is dense inside a solid torus.

References

[AbRo] U. Abresch, H. Rosenberg, Generalized Hopf differentials, *Mat. Contemp.* **28** (2005), 1–28.

[Ale] A.D. Alexandrov, Uniqueness theorems for surfaces in the large, I, *Vestnik Leningrad Univ.* **11** (1956), 5–17. (English translation): Amer. Math. Soc. Transl. **21** (1962), 341–354.

[Bue1] A. Bueno, Half-space theorems for properly immersed surfaces in $\mathbb{R}^3$ with prescribed mean curvature, *Ann. Mat. Pur. Appl.* **199** (2020), 425–444.

[Bue2] A. Bueno, A Delaunay-type classification result for prescribed mean curvature surfaces in $\mathbb{M}^2(\kappa) \times \mathbb{R}$, *Pacific J. Math.* **313** (2021), 45–74.

[Bue3] A. Bueno, Delaunay surfaces of prescribed mean curvature in Nil_3 and $\widetilde{SL_2}(\mathbb{R})$, preprint, arXiv:2003.13018.

[BGM1] A. Bueno, J.A. Gálvez, P. Mira, Rotational hypersurfaces of prescribed mean curvature, *J. Differential Equations* **268** (2020), 2394–2413.

[BGM2] A. Bueno, J.A. Gálvez, P. Mira, The global geometry of surfaces with prescribed mean curvature in $\mathbb{R}^3$, *Trans. Amer. Math. Soc.* **373** (2020), 4437-4467.

[BuOr] A. Bueno, I. Ortiz, Invariant hypersurfaces with linear prescribed mean curvature, *J. Math. Anal. Appl.* **487** (2020), 124033.

[Dan] B. Daniel, Isometric immersions into 3-dimensional homogeneous manifolds, *Comment. Math. Helv.* **82** (2007), 87–131.

[dCFe] M. do Carmo, I. Fernández. A Hopf theorem for open surfaces in product spaces, *Forum Math.* **21** (2009), 951–963.

[DHM] B. Daniel, L. Hauswirth, P. Mira, Constant mean curvature surfaces in homogeneous manifolds, Korea Institute for Advanced Study, Seoul, Korea, 2009.

[FeMi] I. Fernández, P. Mira, Constant mean curvature surfaces in 3-dimensional Thurston geometries. In *Proceedings of the International Congress of Mathematicians*, Volume II (Invited Conferences), pages 830–861. Hindustan Book Agency, New Delhi, 2010.

[FMP] C. B. Figueroa, F. Mercuri and R.H.L. Pedrosa. Invariant surfaces of the Heisenberg groups. *Ann. Mat. Pura Appl.* **177** (1999), 173–194.

[HsHs] W. T. Hsiang, W. Y. Hsiang, On the uniqueness of isoperimetric solutions and imbedded soap bubbles in non-compact symmetric spaces, *Invent. Math.* **85** (1989), 39–58.

[GaMi] J.A. Gálvez, P. Mira, Rotational symmetry of Weingarten spheres in homogeneous three-manifolds, *J. Reine Angew. Math.* **773** (2021), 21–66.

[Gor] C. Gorodski, Delaunay-type surfaces in the 2×2 real unimodular group, *Annali di Matematica.* **180** (2001), 211–221.

[Min] H. Minkowski, Volumen und Oberfläche, *Math. Ann.* **57** (1903), 447–495.

[PeRi] R. H. L. Pedrosa, M. Ritoré, Isoperimetric domains in the Riemannian product of a circle with a simply connected space form and applications to free boundary problems, *Indiana Univ. Math. J.* **48** (1999), 1357–1394.

[Pog] A.V. Pogorelov, Extension of a general uniqueness theorem of A.D. Aleksandrov to the case of nonanalytic surfaces (in Russian), *Doklady Akad. Nauk SSSR* **62** (1948), 297–299.

[Tom] P. Tomter, Constant mean curvature surfaces in the Heisenberg group. *Proc. Sympos. Pure Math.* **54** (1993), 485–495.

[Tor] F. Torralbo, Rotationally invariant constant mean curvature surfaces in homogeneous 3-manifolds. *Diff. Geo. Appl.* **28** (2010), 593–607.

The author was partially supported by P18-FR-4049.